Title

Long-range acoustic observations of the Eyjafjallajökull eruption, Iceland, April-May 2010

Journal

Geophys. Res. Lett., 38

Authors

Matoza, Robin S

Vergoz, Julien

Le Pichon, Alexis

et al.

Publication Date

2011-03-30

Peer reviewed

Long-range acoustic observations of the Eyjafjallajökull eruption, Iceland, April–May 2010

Robin S. Matoza,[1] Julien Vergoz,[1] Alexis Le Pichon,[1] Lars Ceranna,[2] David N. Green,[3] Läslo G. Evers,[4,5] Maurizio Ripepe,[6] Paola Campus,[6] Ludwik Liszka,[7] Tormod Kvaerna,[8] Einar Kjartansson,[9] and Ármann Höskuldsson[10]

Received 7 February 2011; revised 2 March 2011; accepted 7 March 2011; published 30 March 2011.

[1] The April–May 2010 summit eruption of Eyjafjallajökull, Iceland, was recorded by 14 atmospheric infrasound sensor arrays at ranges between 1,700 and 3,700 km, indicating that infrasound from modest-size eruptions can propagate for thousands of kilometers in atmospheric waveguides. Although variations in both atmospheric propagation conditions and background noise levels at the sensors generate fluctuations in signal-to-noise ratios and signal detectability, array processing techniques successfully discriminate between volcanic infrasound and ambient coherent and incoherent noise. The current global infrasound network is significantly more dense and sensitive than any previously operated network and signals from large volcanic explosions are routinely recorded. Because volcanic infrasound is generated during the explosive release of fluid into the atmosphere, it is a strong indicator that an eruption has occurred. Therefore, long-range infrasonic monitoring may aid volcanic explosion detection by complementing other monitoring technologies, especially in remote regions with sparse ground-based instrument networks.
Citation: Matoza, R. S., et al. (2011), Long-range acoustic observations of the Eyjafjallajökull eruption, Iceland, April–May 2010, *Geophys. Res. Lett.*, *38*, L06308, doi:10.1029/2011GL047019.

1. Introduction

[2] Volcanic ash from the April–May 2010 summit eruption of Eyjafjallajökull, Iceland, had a significant societal impact, highlighting the need for effective ash cloud monitoring [*Ansmann et al.*, 2010; *Gudmundsson et al.*, 2010; *Sigmundsson et al.*, 2010]. Ash cloud monitoring involves combining satellite observations and volcano observatory and pilot reports, with weather prediction, ash transport and dispersal forecast models [*Prata and Tupper*, 2009; *Webley and Mastin*, 2009]. The parameters of the volcanic source, such as timing and duration of eruptive activity, are important parameters for ash cloud forecasts [*Prata and Tupper*, 2009; *Webley and Mastin*, 2009]. Multiple dedicated instruments deployed on or near a volcano can be used to monitor eruptive activity [e.g., *McNutt and Nishimura*, 2008; *Moran et al.*, 2008; *Ripepe and Harris*, 2008]. However, many of the world's potentially active volcanoes are not equipped with dedicated monitoring instruments [*Webley and Mastin*, 2009].

[3] Volcanic eruptions are typically a significant source of low-frequency sound radiated directly into the atmosphere [e.g., *Firstov and Kravchenko*, 1996; *Morrissey and Chouet*, 1997; *Liszka and Garces*, 2002; *Johnson*, 2007; *Matoza et al.*, 2009; *Ripepe et al.*, 2010]. During explosive volcanic eruptions, release of conduit overpressure and rapid, sustained and turbulent injection of mass into the atmosphere are the primary sources of low-frequency sound [e.g., *Johnson*, 2007; *Matoza et al.*, 2009; *Fee et al.*, 2010a; *Ripepe et al.*, 2010]. The resulting acoustic waves with frequencies ~0.01–20 Hz, or *infrasound*, can propagate over large distances in the atmosphere due to low attenuation [*Sutherland and Bass*, 2004].

[4] Long-range infrasound propagation takes place primarily in waveguides formed by vertical gradients in temperature and horizontal wind [*Drob et al.*, 2003]. Infrasonic waveguides commonly result from refraction in the troposphere (altitude < ~16 km a.s.l.), in the upper stratosphere (40–55 km a.s.l.), and from within the lower thermosphere (110–160 km a.s.l.) [*Drob et al.*, 2003]. Due to the long-range propagation capabilities of infrasound, several studies have pointed out the utility of infrasonic observations for regional or global-scale volcanic monitoring [*Kamo et al.*, 1994; *Garcés et al.*, 2008; *Fee et al.*, 2010a].

[5] When dedicated monitoring instruments are deployed at a volcano, local or long-range infrasonic observations are a complement, reducing ambiguity in explosion detection [*Matoza et al.*, 2007; *Moran et al.*, 2008; *Ripepe and Harris*, 2008; *Fee et al.*, 2010a]. However, for volcanoes in remote areas without dedicated instruments, long-range infrasonic observations may be the only ground-based observations available to aid interpretation of satellite data and constrain ash dispersal models [*Matoza et al.*, 2011]. For example, no seismic network was in place on Sarychev Peak, Kurils, when it erupted in June 2009 and remote seismic stations at distances >350 km did not record the eruption. However, infrasound was recorded at ranges of 640–6,400 km from Sarychev Peak [*Matoza et al.*, 2011]. We emphasize that the

[1]CEA/DAM/DIF, Arpajon, France.
[2]BGR, Hannover, Germany.
[3]AWE Blacknest, Reading, UK.
[4]Royal Netherlands Meteorological Institute, De Bilt, Netherlands.
[5]Faculty of Aerospace Engineering, Acoustic Remote Sensing, Delft University of Technology, Delft, Netherlands.
[6]Dipartimento Scienze della Terra, Università di Firenze, Firenze, Italy.
[7]Swedish Institute for Space Physics, Umea, Sweden.
[8]NORSAR, Kjeller, Norway.
[9]Icelandic Meteorological Office, Reykjavík, Iceland.
[10]Institute of Earth Sciences, University of Iceland, Reykjavík, Iceland.

0094-8276/11/2011GL047019

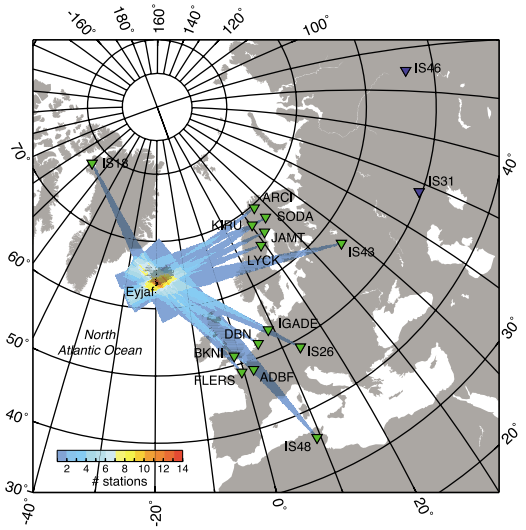

Figure 1. Location of infrasonic stations recording the April–May 2010 summit eruption of Eyjafjallajökull. 14 remote infrasonic arrays (green inverted triangles) recorded the summit eruption of Eyjafjallajökull (black dot, 'Eyjaf'), at distances from ~1,745 km (BKNI, UK) to ~3,666 km (IS48, Tunisia). Blue inverted triangles show other IMS stations that did not record the eruption. Color-scale represents number of intersecting mean infrasonic signal backazimuths ±3° registered at each station and associated with Eyjafjallajökull.

2010 eruption of Eyjafjallajökull was well-monitored by the Icelandic Meteorological Office (IMO) using multiple geophysical and geological data streams [*Gudmundsson et al.*, 2010; *Sigmundsson et al.*, 2010]. In this paper, we identify the exceptional long-range propagation of infrasonic signals from Eyjafjallajökull and use this to illustrate the potential of infrasonic data for use in detecting eruptions at other volcanoes where ground observations are more sparse.

2. Data: Infrasonic Arrays

[6] Infrasonic research has seen a significant resurgence since the Comprehensive Nuclear-Test-Ban Treaty (CTBT) was opened for signature in 1996 and there are currently hundreds of infrasonic sensors deployed globally. The International Monitoring System (IMS) infrasonic network, designed to ensure compliance with the CTBT, already consists of 42 certified stations out of a planned total 60 stations and volcanic signals are detected routinely by this network [*Christie and Campus*, 2010; *Campus and Christie*, 2010]. Figure 1 shows 14 infrasonic arrays that detected the April–May 2010 eruption of Eyjafjallajökull. Some of these arrays (IS18, IS26, IS43, IS48) are stations of the IMS infrasonic network. The remaining arrays (BKNI, LYCK, KIRU, DBN, JAMT, IGADE, FLERS, ARCI, SODA, ADBF) are operated by various European institutions for basic research.

[7] Each infrasonic array consists of at least 3 separate microbarometer or microphone sensor elements connected to a central recording facility. The arrays have apertures ranging from ~75 m up to ~2.5 km. Arrays are used in infrasonic data collection to 1) enable identification of coherent acoustic signals within incoherent background noise (e.g., wind noise) and to 2) allow discrimination between signals of interest and additional coherent infrasound using the signal wavefront properties (e.g., backazimuth, trace-velocity, signal frequency).

3. Observations

3.1. Array Processing

[8] Figure 2a shows coherent infrasonic detections at each recording array that are associated with Eyjafjallajökull. Coherent infrasonic detections were determined using the Progressive Multi-Channel Correlation (PMCC) algorithm [*Cansi*, 1995]. PMCC estimates wavefront properties of coherent acoustic energy as a function of time at an array by considering correlation time-delays between successive array element triplets. We use these estimated wavefront properties to associate the coherent detections to a particular source and to discriminate between different sources, which is important for infrasonic data processing as a large number of natural and man-made infrasonic sources exist.

[9] In particular, *microbaroms* [*Waxler and Gilbert*, 2006] are a significant source of ambient infrasound. Microbaroms, analogous to microseisms recorded by seismometers, are

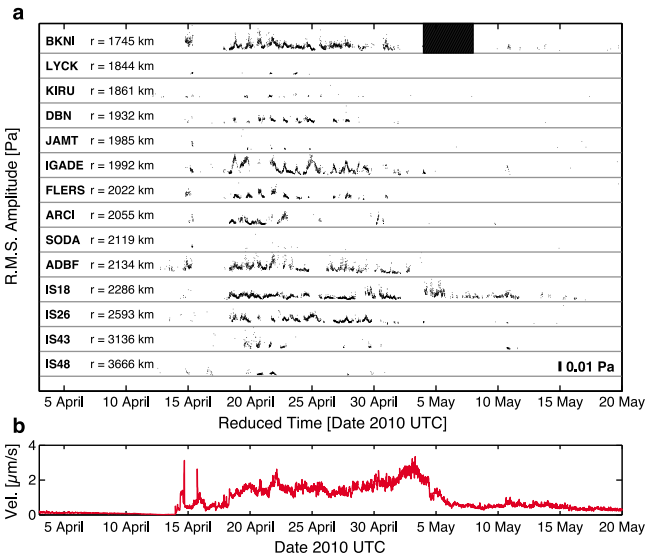

Figure 2. Summary of remote infrasonic array detections compared to local seismic data. (a) Infrasonic station names are consistent with Figure 1. Each panel represents detections at one station (array), with stations shown in order of increasing range from Eyjafjallajökull. Observed detection time is reduced with the approximate travel time of infrasound propagating in the stratosphere (average propagation velocity, or celerity, 0.3 km/s). Y-scale corresponds to 5-minute median averages of the root-mean-square (r.m.s.) amplitude of coherent PMCC detections associated with Eyjafjallajökull. Crosshatched box indicates data gap at BKNI. There are differences in infrasonic sensor response and sampling frequencies between stations. (b) 15-minute median of seismic vertical velocity amplitude at station MID filtered between 1 and 2 Hz, ~14 km from the summit of Eyjafjallajökull.

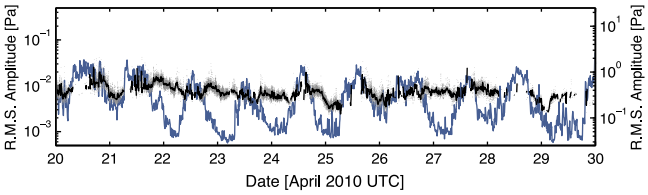

Figure 3. Signal and noise amplitude variations at BKNI, UK. PMCC detection r.m.s. amplitudes (gray dots, left-hand scale) and their 10-minute median values (black line, left-hand scale) indicate coherent acoustic detections associated with Eyjafjallajökull. This is compared to r.m.s. amplitude of raw pressure at one element of the BKNI array in the 0.01–0.5 Hz band (blue line, right-hand scale).

generated by non-linear wave-wave interaction in the open ocean [*Waxler and Gilbert*, 2006]. The North Atlantic Ocean around Iceland (see Figure 1) is a significant microbarom source region. Consequently, signals from Eyjafjallajökull and microbaroms arrived from similar azimuths at most of the stations. Discrimination between microbaroms and signals from Eyjafjallajökull was achieved at each station using an empirical procedure based on the statistical distributions of estimated wavefront properties (backazimuth, trace-velocity and mean signal frequency). For instance, microbaroms have lower-frequency content (~0.2 Hz), whereas the volcanic detections have higher frequencies (~0.5–4 Hz). Detections shown on Figure 2 represent detections associated with Eyjafjallajökull with a probability of 90%, and ~10% of detections shown on Figure 2a are attributed to other sources (mostly microbaroms).

3.2. Comparison With Local Seismic Data

[10] The explosive summit eruption of Eyjafjallajökull began on 14 April 2010, preceded by an effusive flank eruption from 20 March to 12 April 2010 [*Gudmundsson et al.*, 2010; *Sigmundsson et al.*, 2010]. No long-range infrasound was detected from the flank eruption, consistent with the lack of explosive activity. A near-continuous series of long-range infrasonic detections delineate the timing of the summit eruption, as confirmed by comparing with local IMO seismic data (Figure 2b).

[11] An initial burst of infrasonic detections is observed on 14 and 15 April 2010 (Figure 2a), immediately following an increase in locally recorded 15-minute averaged seismic amplitude, a measure of continuous ground-shaking or *tremor* (Figure 2b). This is followed by repose in detected infrasound between 15–17 April at most stations, suggesting low-amplitude infrasonic source activity. During this time, local seismic tremor is continuous but with amplitude lower than maximum values during 14–15 April (Figure 2b). From 18 April, infrasonic signals are recorded quasi-continuously before waning at all stations by 20 May. This coincides broadly with local seismic observations: seismic tremor increases on 18 April, remains sustained at high amplitude until ~5 May, and wanes to low values by 20 May. However, we note that seismic tremor amplitude reaches a maximum between 2 and 4 May. This corresponds to a time when very few infrasonic detections are recorded, suggestive of variable seismic-acoustic source partitioning.

[12] Variable seismic-acoustic energy partitioning has been observed previously in dedicated volcano seismo-acoustic studies [e.g., *Johnson and Aster*, 2005; *Matoza et al.*, 2007]. Generally, variable seismic-acoustic energy partitioning occurs because volcano seismic signals can be generated at a range of depths in the subsurface, while volcano acoustic signals require a source well-coupled to the atmosphere [e.g., *Ripepe et al.*, 2009]. However, the reduction in infrasonic detections between 15–17 April and during 2–4 May could also be related to changes in atmospheric propagation.

3.3. Atmospheric Propagation and Signal Detectability

[13] The recorded amplitude variations of infrasonic signals as a function of time in Figure 2a represent the end result of a convolution between time-dependent source amplitude and time-dependent atmospheric propagation effects. The time series are also modified by the time-dependent ability of the station to detect signals. In particular, prominent diurnal variations of the signal detectability and r.m.s. (root-mean-square) amplitude (Figures 2a and 3) can be attributed to both diurnal changes in the station background noise levels and to diurnal changes in the state of the atmosphere along the principal stratospheric propagation path between Eyjafjallajökull and each station.

[14] Figure 3 shows the r.m.s. amplitude of PMCC detections at BKNI from 20 to 30 April 2010 (gray dots and black line). Also shown is pressure amplitude in the band 0.01–0.5 Hz (blue line), a useful proxy for incoherent wind noise at an array [*Fee and Garcés*, 2007]. Incoherent wind noise increases significantly during the daytime due to increased turbulence in the atmospheric boundary layer [*Fee and Garcés*, 2007]. Wind noise is concentrated at low frequencies (0.01–0.5 Hz) but extends into the higher frequency band (0.5–5 Hz). Increases in incoherent wind noise are marked by increases in noise in the 0.01–0.5 Hz band (blue line). During these times, infrasonic detections (gray dots, black lines) are generally diminished. Thus, wind noise can explain much of the diurnal variation in signal detectability at each array (Figures 2a and 3).

[15] Other features of the amplitude variations in Figure 2a, such as the cyclic diurnal amplitude variations, are attributable to long-range propagation characteristics of infrasound in the stratosphere. Ongoing research on infrasound propagation in a dynamic atmosphere and infrasonic network detection capability studies are leading to significant improvements in our understanding of atmospheric infrasound propagation and detectability [*Le Pichon et al.*, 2008, 2009].

4. Discussion: Utility of Long-Range Volcanic Infrasound

[16] Despite variations in signal detectability (Figure 3), resulting in periods of low-signal-to-noise ratios, the recorded signals provide a useful tool for monitoring remote explosive volcanism and associated ash plumes. Intersection of mean signal backazimuths projected back from each station results in a source location estimate (Figure 1). The mean centroid of maximum intersection falls ~50 km north of the true location of Eyjafjallajökull. The source location, together with signal onset time and duration, could be estimated quickly and automatically for combination with

satellite data and ash dispersal models. Accuracy of source location estimates may be improved by adding corrections for azimuth deviation caused by wind components perpendicular to the direction of propagation. Improving the accuracy of source location estimates increases the likelihood of correctly identifying which volcano has erupted, especially when multiple potentially active volcanoes are in proximity.

[17] Larger volcanic explosions will usually produce higher signal-to-noise ratio recordings, and signal-to-noise ratio will improve with reduced source-receiver range. For instance, the June 2009 eruption of Sarychev Peak [*Matoza et al.*, 2011] produced maximum r.m.s. signal amplitudes of ~0.4 Pa at 643 km and ~0.25 Pa at 1,690 km in comparison to the max r.m.s. amplitude of ~0.03 Pa recorded at 1,745 km (BKNI) from Eyjafjallajökull (Figure 3). As the signal-to-noise ratio increases, more detailed analysis and interpretation is possible. For instance, the acoustic pressure r.m.s. amplitude of long-range infrasound from Eyjafjallajökull (Figures 2a and 3) cannot be related unambiguously to eruptive intensity. However, at closer ranges (~10–40 km), acoustic energy of broadband infrasound radiated by sustained vulcanian and plinian eruptions appears to scale with eruptive intensity and ash column height [*Fee et al.*, 2010a].

[18] Furthermore, detailed source process models are being developed that may enable the flow parameters feeding volcanic eruption columns to be inferred from radiated infrasound properties (e.g., the source spectrum) [*Garcés et al.*, 2008; *Matoza et al.*, 2009; *Fee et al.*, 2010a, 2010b]. Coupled with accurate infrasonic propagation modeling, this could enable more detailed constraints on volcanic eruption column parameters using high signal-to-noise ratio recordings of long-range infrasound [*Garcés et al.*, 2008; *Matoza et al.*, 2009; *Fee et al.*, 2010a, 2010b].

5. Conclusions

[19] The April–May 2010 summit eruption of Eyjafjallajökull produced significant infrasound, which propagated through the atmosphere greater than ~3,500 km from the volcano. The overall timing of the infrasonic signal reception correlates well with the duration of the summit eruption determined from local observations (e.g., local seismic data, Figure 2b). No infrasound was detected from the preceding non-explosive flank eruption (20 March to 12 April 2010), consistent with infrasound being generated primarily from explosive activity. Variations in background noise levels at the arrays and atmospheric propagation cause noticeable fluctuations in signal-to-noise ratios and signal detectability at long ranges from Eyjafjallajökull. Nevertheless, the long-range propagation capability of infrasound is remarkable. In more remote regions of the planet (not monitored by dedicated instruments), some volcanoes have the potential to erupt with greater explosive energy than Eyjafjallajökull and inject greater volumes of ash into heavily travelled air corridors. In such situations, infrasonic data may serve as a critical complement to other volcano monitoring technologies.

[20] **Acknowledgments.** We thank P. Gaillard for help with event discrimination, and D. Fee and E. Marchetti for comments on the paper. The paper was improved after a careful review by P. Webley.

[21] The Editor thanks Peter Webley and an anonymous reviewer for their assistance in evaluating this paper.

References

Ansmann, A., et al. (2010), The 16 April 2010 major volcanic ash plume over central Europe: EARLINET lidar and AERONET photometer observations at Leipzig and Munich, Germany, *Geophys. Res. Lett.*, *37*, L13810, doi:10.1029/2010GL043809.

Campus, P., and D. R. Christie (2010), Worldwide observations of infrasonic waves, in *Infrasound Monitoring for Atmospheric Studies*, edited by A. Le Pichon et al., pp. 185–234, Springer, Dordrecht, Netherlands, doi:10.1007/978-1-4020-9508-5_6.

Cansi, Y. (1995), An automatic seismic event processing for detection and location: The PMCC method, *Geophys. Res. Lett.*, *22*(9), 1021–1024, doi:10.1029/95GL00468.

Christie, D. R., and P. Campus (2010), The IMS infrasound network: Design and establishment of infrasound stations, in *Infrasound Monitoring for Atmospheric Studies*, edited by A. Le Pichon et al., pp. 29–75, Springer, Dordrecht, Netherlands, doi:10.1007/978-1-4020-9508-5_2.

Drob, D. P., J. M. Picone, and M. Garcés (2003), Global morphology of infrasound propagation, *J. Geophys. Res.*, *108*(D21), 4680, doi:10.1029/2002JD003307.

Fee, D., and M. Garcés (2007), Infrasonic tremor in the diffraction zone, *Geophys. Res. Lett.*, *34*, L16826, doi:10.1029/2007GL030616.

Fee, D., et al. (2010a), Infrasound from Tungurahua Volcano 2006–2008: Strombolian to plinian eruptive activity, *J. Volcanol. Geotherm. Res.*, *193*(1–2), 67–81, doi:10.1016/j.jvolgeores.2010.03.006.

Fee, D., A. Steffke, and M. Garcés (2010b), Characterization of the 2008 Kasatochi and Okmok eruptions using remote infrasound arrays, *J. Geophys. Res.*, *115*, D00L10, doi:10.1029/2009JD013621.

Firstov, P. P., and N. M. Kravchenko (1996), Estimation of the amount of explosive gas released in volcanic eruptions using air waves, *Volcanol. Seismol.*, *17*, 547–560.

Garcés, M., et al. (2008), Capturing the acoustic fingerprint of stratospheric ash injection, *Eos Trans. AGU*, *89*(40), 377–379, doi:10.1029/2008EO400001.

Gudmundsson, M. T., et al. (2010), Eruptions of Eyjafjallajökull Volcano, Iceland, *Eos Trans. AGU*, *91*(21), 190, doi:10.1029/2010EO210002.

Johnson, J. B. (2007), On the relation between infrasound, seismicity, and small pyroclastic explosions at Karymsky volcano, *J. Geophys. Res.*, *112*, B08203, doi:10.1029/2006JB004654.

Johnson, J. B., and R. C. Aster (2005), Relative partitioning of acoustic and seismic energy during Strombolian eruptions, *J. Volcanol. Geotherm. Res.*, *148*(3–4), 334–354, doi:10.1016/j.jvolgeores.2005.05.002.

Kamo, K., et al. (1994), Infrasonic and seismic detection of explosive eruptions at Sakurajima volcano, Japan, and the PEGASAS-VE early-warning system, in *Volcanic Ash and Aviation Safety: Proceedings of the First International Symposium on Volcanic Ash and Aviation Safety*, edited by T. J. Casadevall, *U.S. Geol. Surv. Bull.*, *2047*, 357–365.

Le Pichon, A., J. Vergoz, P. Herry, and L. Ceranna (2008), Analyzing the detection capability of infrasound arrays in central Europe, *J. Geophys. Res.*, *113*, D12115, doi:10.1029/2007JD009509.

Le Pichon, A., J. Vergoz, E. Blanc, J. Guilbert, L. Ceranna, L. Evers, and N. Brachet (2009), Assessing the performance of the International Monitoring System's infrasound network: Geographical coverage and temporal variabilities, *J. Geophys. Res.*, *114*, D08112, doi:10.1029/2008JD010907.

Liszka, L., and M. A. Garces (2002), Infrasonic observations of the Hekla eruption of February 26, 2000, *J. Low Frequation Noise Vib. Act. Control*, *21*(1), 1–8, doi:10.1260/02630920260374934.

Matoza, R. S., et al. (2007), An infrasound array study of Mount St. Helens, *J. Volcanol. Geotherm. Res.*, *160*(3–4), 249–262, doi:10.1016/j.jvolgeores.2006.10.006.

Matoza, R. S., D. Fee, M. A. Garcés, J. M. Seiner, P. A. Ramón, and M. A. H. Hedlin (2009), Infrasonic jet noise from volcanic eruptions, *Geophys. Res. Lett.*, *36*, L08303, doi:10.1029/2008GL036486.

Matoza, R. S., et al. (2011), Infrasonic observations of the June 2009 Sarychev Peak eruption, Kuril Islands: Implications for infrasonic monitoring of remote explosive volcanism, *J. Volcanol. Geotherm. Res.*, *200*(1–2), 35–48, doi:10.1016/j.jvolgeores.2010.11.022.

McNutt, S. R., and T. Nishimura (2008), Volcanic tremor during eruptions: Temporal characteristics, scaling and constraints on conduit size and processes, *J. Volcanol. Geotherm. Res.*, *178*(1), 10–18, doi:10.1016/j.jvolgeores.2008.03.010.

Moran, S. C., et al. (2008), Seismicity and infrasound associated with explosions at Mount St. Helens, in *A Volcano Rekindled: The Renewed Eruption of Mount St. Helens, 2004–2006*, edited by D. R. Sherrod et al., Chapter 6, *U.S. Geol. Surv. Prof. Pap.*, *1750*, 111–128.

Morrissey, M. M., and B. A. Chouet (1997), Burst conditions of explosive volcanic eruptions recorded on microbarographs, *Science*, *275*(5304), 1290–1293, doi:10.1126/science.275.5304.1290.

Prata, A. J., and A. Tupper (2009), Aviation hazards from volcanoes: The state of the science, *Nat. Hazards*, *51*(2), 239–244, doi:10.1007/s11069-009-9415-y.

Ripepe, M., and A. J. L. Harris (2008), Dynamics of the 5 April 2003 explosive paroxysm observed at Stromboli by a near-vent thermal, seismic and infrasonic array, *Geophys. Res. Lett.*, *35*, L07306, doi:10.1029/2007GL032533.

Ripepe, M., et al. (2009), The onset of the 2007 Stromboli effusive eruption recorded by an integrated geophysical network, *J. Volcanol. Geotherm. Res.*, *182*(3–4), 131–136, doi:10.1016/j.jvolgeores.2009.02.011.

Ripepe, M., S. De Angelis, G. Lacanna, and B. Voight (2010), Observation of infrasonic and gravity waves at Soufrière Hills Volcano, Montserrat, *Geophys. Res. Lett.*, *37*, L00E14, doi:10.1029/2010GL042557.

Sigmundsson, F., et al. (2010), Intrusion triggering of the 2010 Eyjafjallajökull explosive eruption, *Nature*, *468*(7322), 426–430, doi:10.1038/nature09558.

Sutherland, L. C., and H. E. Bass (2004), Atmospheric absorption in the atmosphere up to 160 km, *J. Acoust. Soc. Am.*, *115*(3), 1012–1032, doi:10.1121/1.1631937.

Waxler, R., and K. E. Gilbert (2006), The radiation of atmospheric microbaroms by ocean waves, *J. Acoust. Soc. Am.*, *119*(5), 2651–2664, doi:10.1121/1.2191607.

Webley, P., and L. Mastin (2009), Improved prediction and tracking of volcanic ash clouds, *J. Volcanol. Geotherm. Res.*, *186*(1–2), 1–9, doi:10.1016/j.jvolgeores.2008.10.022.

P. Campus and M. Ripepe, Dipartimento Scienze della Terra, Università di Firenze, I-50121 Firenze, Italy.

L. Ceranna, BGR, Stilleweg 2, D-30655 Hannover, Germany.

L. G. Evers, Royal Netherlands Meteorological Institute, NL-3730 AE De Bilt, Netherlands.

D. N. Green, AWE Blacknest, Reading RG7 4RS, UK.

Á. Höskuldsson, Institute of Earth Sciences, University of Iceland, Sturlugata 7, 101 Reykjavík, Iceland.

E. Kjartansson, Icelandic Meteorological Office, Bústaðavegi 9, 150 Reykjavík, Iceland.

T. Kvaerna, NORSAR, Post Box 53, N-2007 Kjeller, Norway.

A. Le Pichon, R. S. Matoza, and J. Vergoz, CEA/DAM/DIF, F-91297 Arpajon, France. (robin.matoza@cea.fr)

L. Liszka, Swedish Institute for Space Physics, Teknikhuset, SE-901 87 Umea, Sweden.